Mitig Adapt Strat Glob Change (2008) 13:437–451
DOI 10.1007/s11027-007-9130-5

ORIGINAL ARTICLE

Coastal flooding in the Northeastern United States due to climate change

Paul Kirshen · Chris Watson · Ellen Douglas · Allen Gontz · Jawon Lee · Yong Tian

Received: 12 December 2006 / Accepted: 30 May 2007 / Published online: 4 December 2007

Abstract With dense population and development along its coastline, the northeastern United States is, at present, highly vulnerable to coastal flooding. At five sea level stations in the United States, from Massachusetts to New Jersey, sea level rise (SLR) trends and tidal effects were removed from the hourly sea level time series and then frequency analysis was performed on the positive remaining anomalies that represent storm surge heights. Then using eustatic SLR estimates for lower and higher greenhouse gas emissions scenarios and assumed trends in local sea level rise, new recurrence intervals were determined for future storm surges. Under the higher emissions scenario, by 2050, the elevation of the 2005 100-year event may be equaled or exceeded at least every 30 years at all sites. In more exposed US cities such as Boston, Massachusetts and Atlantic City, New Jersey, this could occur at the considerably higher frequency of every 8 years or less. Under the lower emissions scenario, by 2050, the elevation of the 2005 100-year event may be equaled or exceeded at least every 70 years at all sites. In Boston and Atlantic City, this could occur every 30 years or less.

Keywords Climate change · Sea level rise · Storm surge · Coastal flooding · Recurrence of severe coastal flooding events · United States · Greenhouse gas emissions · Massachusetts · Connecticut · New York · New Jersey

1 Introduction

The United Nations Intergovernmental Panel on Climate Change (IPCC) Fourth Assessment Report states that "most of the observed increase in globally averaged temperatures since the mid-20th century is very likely due to the observed increase in anthropogenic greenhouse gas

P. Kirshen (✉)
Civil and Environmental Engineering Department and Water: Systems, Science, and Society Research and Graduate Education Program, Tufts University, Medford, MA 01742, USA
e-mail: paul.kirshen@tufts.edu

C. Watson · E. Douglas · A. Gontz · J. Lee · Y. Tian
Environmental, Earth and Ocean Sciences Department, University of Massachusetts, Boston, MA 02125, USA

concentrations (Summary for Policy Makers, Working Group 1 [WG 1] IPCC 2007, p. 10). One of the impacts of this warming has been an increase in sea level because of the melting of ice on land and thermal expansion of the ocean. The sum of these two effects is known as eustatic sea level rise (SLR, Pugh 2004). A recent calculation using the quadratic fitted reconstructed SLR data derived from the Topex/Poseidon (T/P) altimeter and other data sets provides an estimate of eustatic SLR from 1880 to 2000 of 1.6 mm/year (Bindoff and Willebrand 2007). This value falls within the range of another recent estimate derived from the T/P dataset combined with other data of 1.8±0.3 mm/year for the period 1950 to 2000 (Church et al. 2004). The research of Holgate and Woodworth (2004) indicates that the rate of eustatic coastal SLR in the late 20th century is greater than the average eustatic SLR in the second half of the 20th century.

Sea level elevation relative to land is also related to processes that affect a specific region, including tectonic uplift and down dropping, isostatic rebound and depression, land surface changes due to compaction, dewatering, fluid extraction, and diagenetic processes. For example, in coastal Boston, Massachusetts in the northeastern United States, land subsidence is estimated by Nucci Vine Associates, Inc. (1992) to have been 1.5 mm/year or 0.15 m in the last 100 years. An estimate of 2 mm/year for historical subsidence in Revere, near the north of Boston, was reported in Clark et al. (1998). We define these effects as local SLR. Eustatic SLR combined with local SLR is referred to as relative SLR. Church and Gregory (2001) reported that the rate of global mean relative SLR over the last 100 years has been 1.0 to 2.0 mm/year. The effects of relative SLR in the coastal zone include displacement and loss of wetlands, inundation of low-lying property, increased erosion of the shoreline, changes in the extent of flood zones, changing water circulation patterns, and more salt water intrusion into groundwater and estuaries. Recent scenarios from Hayhoe (personal communication 2006) discussed in Section 2.4 give a 2000 to 2100 range of eustatic SLR of 1.2 mm/year to 8.4 mm/year, depending on the emissions scenario chosen. Climate change could also result in changes in coastal hurricane storm patterns that alter the frequency and intensity of coastal flooding (Emanuel 2005), exacerbating the impacts of relative SLR already mentioned. These additional impacts were not considered.

In this study, we estimate the change in recurrence intervals of storm surges in the northeastern United States due to possible SLR scenarios. We also compare the boundaries of a 100-year coastal storm flooding event (i.e., the event that, on average, is expected to be equaled or exceeded once every 100 years or has the probability of 0.01 of being equaled or exceeded each year) in Boston developed by the Federal Emergency Management Agency (FEMA) with the flooding boundaries of our estimated storm surges for 2005 and 2100 to further infer the potential social and economic impacts of climate change on coastal areas.

Coastal flooding in this region of the United States has been very costly in the past. Cooper et al. (2005) report that in the mid-Atlantic region the “Ash Wednesday” coastal storm of March 1962 caused over $500 million in damage and the “Halloween Northeaster” of 1991 resulted in over $1.5 billion in damage. Kirshen et al. (2004) report that the February “Blizzard of 1978” storm caused coastal damages of $550 million and required $95 million in emergency costs in Massachusetts, mainly in metropolitan Boston.

There are several detailed studies of the possible coastal flooding impacts of SLR in the northeastern United States. Rosenzweig and Solecki (2001) produced a study of the impacts of climate change on the New York metropolitan area, which predicted serious impacts to the region’s transportation systems and an increase in the rates of beach erosion, albeit based on older climate models and previous IPCC emissions scenarios. Cooper et al. (2005) determined possible changes in coastal flood frequencies due to SLR in New Jersey and associated increases in floodplains. The US New England Regional Assessment Group

(NERA) performed an analysis of climate change for all of New England and New York and concluded that both low-lying infrastructure and wetlands would be at-risk (NERA 2001). The US Army Corps of Engineers (1990) estimated that the additional flood losses arising from one foot of SLR in the next 100 years to the heavily developed and industrialized Saugus River estuary area directly north of Boston, Massachusetts with a coastline of 8 km would be $1.4 million/year. While not directly examining the impacts of climate change, Clark et al. (1998) showed that physical vulnerability to flooding must be combined with the socio-economic vulnerabilities in coastal flood management in Revere, Massachusetts.

Among the few studies that attempted to evaluate future costs of increased coastal flooding due to climate change and SLR were Kirshen et al. (2004, 2006). They found that depending upon the SLR scenario and the adaptation action taken, cumulative future damages to buildings, building contents, and the associated emergency costs in the metropolitan Boston region could vary from $6 billion to $94 billion with no discounting or inflation in the period 2000 to 2100. Without climate change and with present flood management policies in place the cumulative costs would be approximately $7 billion.

Here we present the results of research carried out at select sites from a larger geographical area with a stronger emphasis on our own statistical analysis of sea-level anomalies. We also used the eustatic SLR estimates from the most current greenhouse gas emissions scenarios and assumed trends in local SLR to determine new recurrence intervals for future storm surges.

2 Methodology

2.1 Data reduction

Sea level data from the Tides and Current web site of the National Oceanic and Atmospheric Administration/National Ocean Service (NOAA/NOS) Center for Operational Oceanographic Products and Services (CO-OPS) were obtained for five sites: Boston, Massachusetts, Woods Hole, Massachusetts, New London, Connecticut, New York, New York, and Atlantic City, New Jersey (NOAA 2007). Datasets from the NOS included both predicted and verified (i.e. actual) hourly water level measurements in meters relative to both the North American Vertical Datum of 1988 (NAVD) and Universal Coordinated Time (Z). We obtained data for the longest period for which reliable data were available. The locations of these sites are shown in Fig. 1 and the attributes are listed in Table 1.

The first step in data reduction involved removing trends in SLR from the raw time series. The linear regression slopes provided by NOAA/NOS (given in Table 1) were used to remove the historical trends in SLR at each station. Theoretical tidal variations from the NOS tide model for each station were then subtracted from the detrended sea level time series. The resulting datasets were defined as sea level anomalies. These detrended sea level anomalies can be expressed as:

$$WLA_{i,t} = WLV_{i,t} - [SLT_i(t - T_{0i})] - WLP_{i,t} \quad (1)$$

where

$WLA_{i,t}$	water-level anomaly (mm)
i	NOS Gauge Station
t	date/time value (hours Z)
SLT_i	NOS sea-level trend (mm/day)
T_{0i}	date/time of zero SLR relative to MSL (days Z)

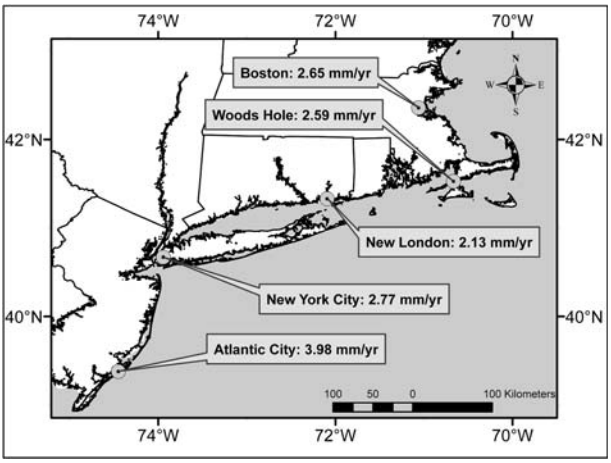

Fig. 1 Study area showing the location of five sea-level gauge stations and associated trend values obtained from the Tides and Currents website of the National Oceanic and Atmospheric Administration/National Ocean Service Center for Operational Oceanographic Products and Services' (http://tidesandcurrents.noaa.gov)

$WLV_{i,t}$ NOS verified water-level measurement (mm NAVD)
$WLP_{i,t}$ NOS predicted water-level or tidal measurement (mm NAVD)

To obtain the SLT_i value in mm/day, the SLT_i value provided by NOS (mm/year, see Table 1) was simply divided by 365 days and therefore does not include corrections for leap years. The incremental SLT_i for each day of the tidal record was subtracted from the hourly values for that day. This results in an overestimation of anomaly heights throughout the day and the correct adjustment at the end of the day. The maximum error is always in the first hour of each day. For example, in Boston, Massachusetts, the maximum error in the first hour of each day is 2.65 mm/year divided by 365 days or 0.0073 mm/day. Since, as stated

Table 1 National Ocean Service Tidal gauge station attributes (location, trends and datums) for each of the sites in the United States evaluated in this study

Station	Boston, Massachusetts	Woods Hole, Massachusetts	New London, Connecticut	New York City, New York	Atlantic City, New Jersey
Latitude North	42° 21.3′	41° 31.4′	41° 21.3′	40° 42.0′	39° 21.3′
Longitude West	71° 3.1′	70° 40.3′	72° 5.2′	74° 0.9′	74° 25.1′
Record length (years)	1921–2005	1958–2005	1938–2005	1920–2005	1920–2005
Data gaps (years)	1942, 1945	None	None	None	1938–58, 79–84
NOS historical relative sea level (RSL) trends					
Trend (mm/year)	2.65	2.59	2.13	2.77	3.98
Standard error (mm/year)	0.10	0.12	0.15	0.05	0.11
Period of analysis (years)	1921–1999	1932–1999	1938–1999	1856–1999	1911–1999
Station datums (meters NAVD)					
Mean sea level (MSL)	−0.093	−0.115	−0.092	−0.064	−0.122
Mean higher high water (MHHW)	1.453	1.469	0.370	0.694	0.606
MHHW-MSL (meters)	1.546	1.584	0.462	0.758	0.728
Local sea level (LSL) calculated factor (mm/year)	1.1	1.0	0.5	1.2	2.4

below, we removed all anomalies less than 25 cm, any error introduced by this approximation did not affect our results.

T_{0i} was estimated from visual observation of the NOS Mean Sea Level Trend plots provided on the NOAA Tides and Currents web site. Additionally, T_{0i} was further approximated by assuming MSL=0.000 mm NAVD (refer to Table 1 for actual values of MSL relative to NAVD). Therefore, for all anomaly calculations and all sites, T_{0i}=January 1, 1983 (the start of the current Tidal Epoch).

NOAA reported that modeled tidal estimates are accurate to within 0.6 ft (19 cm). We selected a threshold of 25 cm to remove positive anomalies that could be attributed to model error. Negative anomalies were not evaluated in this study. This 25 cm threshold was applied to each time series of sea level anomalies to create a "points-over-threshold" (POT) anomaly time series. POT anomalies that exceeded the 25 cm threshold were assumed to represent the height of a "storm", "coastal flooding", or "storm surge" event. Cluster analysis was performed on the POT anomaly time series to remove multiple anomalies from the same storm. To do this, we assumed a minimum 24-h period between storms; hence POT anomalies that were less than 24 h apart were assumed to be generated by the same storm. We selected the maximum of these within-storm anomalies to represent the storm surge height.

2.2 Trend analysis

We anticipated that the POT anomaly time series (which essentially represented filtered residuals from the NOS tidal model) would have no trend. However, we found a strongly increasing trend in the number of anomalies that occurred within each year (Fig. 2). We created annual time series by selecting the maximum anomaly from each year of the POT time series and found that the annual time series at each site also contained an increasing trend, which we quantified by ordinary least squares regression. Table 2 presents the slope of the regression line (in mm/yr) and its p-value and the coefficient of variance (R^2) for the regression.

A p-value less than or equal to 0.025 (two-tailed test) indicates that the regression slope is statistically different than zero at a significance level of 95%. Statistically significant slopes in the annual maximum anomaly time series were observed for two US sites: Atlantic City and Boston. We noted that these two stations were the most exposed sites with respect to ocean storms; Woods Hole, Massachusetts is protected by Buzzards Bay and the New York, New York and New London, Connecticut sites are within Long Island Sound.

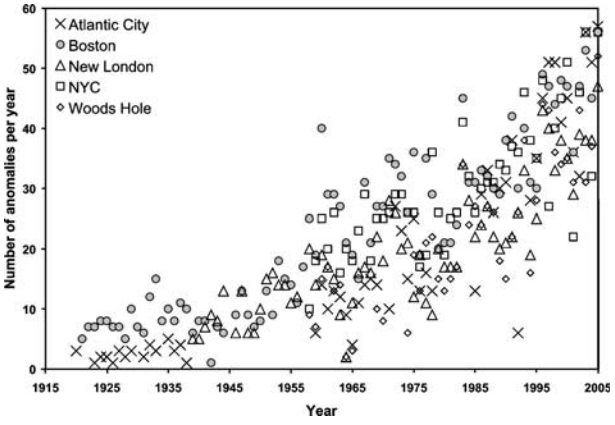

Fig. 2 The number of points-over-threshold (POT) anomalies per year for each site. A strongly increasing trend in the number of POT anomalies was observed at all sites

Table 2 Summary of the regression analysis of annual maximum storm surge anomaly heights for each site, including record length, slope, coefficient of variation (R^2) and statistical significance (as indicated by the *p*-value)

Site	*N*	Slope (mm/year)	R^2	*p*-value
Boston	84	3.20	0.13	0.00
Woods Hole	42	3.02	0.04	0.23
New London	65	2.76	0.03	0.14
New York City	48	3.95	0.03	0.23
Atlantic City	54	7.38	0.46	0.00

A two-sided *p* value less than or equal to 0.025 indicates that the slope is significantly different from zero with 95% statistical confidence.

Zhang et al. (2000) reported no observed trends in the number or intensity of storm surges at these sites. However, in their analysis they removed the tidal component from their sea level time series by developing individual harmonic models for each year; hence, their method inherently accounted for long-term changes in tidal characteristics, whereas ours did not. Therefore, we hypothesized that our observed trends were due, at least in part, to a trend (or trends) in tidal characteristics not accounted for by the NOS tidal model. Flick et al. (1999) analyzed tidal records along the East Coast and found changes in tides that differed by site, and were generally increasing.

2.3 Frequency analysis

Our original intention was to perform frequency analysis on the cluster-filtered POT time series using the Generalized Extreme Value (GEV) distribution as outlined in Section 18.6 of Stedinger et al. (1993) and Thompson et al. (2007). However, the GEV shape parameters (κ) estimated from these POT data were strongly negative and out of range (per Stedinger et al. (1993), κ typically ranges between −0.2 and 0.2). This is likely due to the strongly increasing trend in the number of anomalies, as discussed in Section 2.2. Therefore, we did not believe that a frequency analysis of the POT data would be appropriate at this point. Instead, we elected to perform frequency analysis on the annual maximum anomalies identified at each site. Since we were not able to fully explore the mechanisms behind the trends, we performed frequency analysis on both raw (trend not removed) and detrended time series at the two sites (Atlantic City and Boston) where we found statistically significant slopes in the annual maximum anomaly time series. At the other three sites, frequency analysis was performed on the raw time series only.

The GEV probability distribution function was selected for describing the frequency distribution of the annual maximum anomalies based on our own experience with extreme events (Douglas and Vogel 2006) and based on the use of the GEV in other studies of storm surges (Pugh 2004; van den Brink et al. 2003; Flather and Williams 2000). The GEV parameters were estimated using the method of *L*-moments as described in Stedinger et al. (1993) and Hosking and Wallis (1997). Goodness-of-fit was confirmed using a probability plot correlation coefficient (PPCC) hypothesis test (Chowdhury et al. 1991) and an *L*-moment diagram. A more detailed discussion is included in Appendix A. The GEV parameter estimates for both raw (trend not removed) and detrended time series were computed for Atlantic City and Boston. Estimated storm surge anomaly heights based on the GEV distribution are shown in Table 3. Height estimates from the detrended time series (2nd and 4th columns in Table 3) were adjusted to the contemporary timeframe (2005) by adding in

Table 3 Storm surge anomaly height estimates by recurrence interval using the Generalized Extreme Value (GEV) distribution for each site

Return period (year)	Estimated annual maximum sea level heights (in mm)[a]						
	Boston[b]	Boston[c]	Woods Hole	New London	New York City	Atlantic City[b]	Atlantic City[c]
2	1,017	1,152	757	841	1,030	791	1,051
5	1,197	1,315	948	1,103	1,317	1,060	1,247
10	1,276	1,384	1,085	1,282	1,502	1,207	1,373
20	1,331	1,431	1,224	1,458	1,676	1,329	1,491
50	1,380	1,472	1,416	1,692	1,895	1,464	1,640
100	1,407	1,494	1,570	1,873	2,055	1,549	1,749
200	1,426	1,509	1,731	2,056	2,211	1,624	1,855
500	1,444	1,523	1,959	2,306	2,413	1,707	1,992
1,000	1,453	1,530	2,142	2,500	2,562	1,761	2,092

Because a statistically significant trend in annual maximum anomaly heights was observed at Boston, Massachusetts and Atlantic City, New Jersey, USA, frequency analysis was performed on both raw (trend not removed prior to frequency analysis) and detrended (trend removed prior to frequency analysis) time series for these sites.

[a] GEV parameters estimated from anomaly data in units of meters and later converted to millimeters

[b] Linear trend was not removed prior to estimating GEV parameters

[c] Linear trend was removed prior to estimating GEV parameters

the linear trend as it occurred over the period of record (86 years for Atlantic City, 85 years for Boston). In so doing, we assume that the frequency characteristics of the time series have not changed over time.

We used these results to determine the recurrence intervals of the maximum anomalies that occurred during some well-known coastal storms in the region both at the times of their occurrence and in 2005. As seen in Table 4, the recurrence intervals of all of the anomalies are low with the exception of the "Perfect Storm" on 31 October 1991. Moreover, except for the Blizzard of 1978, the anomalies associated with these storms were not the maximum annual anomalies for those years. These storms were damaging because of the tidal and wave effects that accompanied the anomalies, i.e., the long duration of the storms over several tidal cycles and the onshore winds leading to major flooding and erosion. If such dangerous tidal and wave effects were to occur with larger anomalies, then damages would be greater. As will be shown subsequently, with expected decreases in recurrence intervals of anomalies due to climate change, the probabilities of this occurring are growing as climate change proceeds, and faster under the higher emissions scenario than under the lower one.

2.4 SLR scenarios

We assumed that future local SLR would equal the historical local SLR, which was found by subtracting the eustatic SLR rate of 1.6 mm/year from T/P data set from the relative SLR rate at each station. For example, in Boston, the historical relative SLR is reported to be 2.65 mm/year. Therefore, the historical local SLR in Boston is 2.65 mm/year minus 1.6 mm/year or 1.1 mm/year.

Future scenarios of greenhouse gas emissions from human activities drive temperature changes (Nakicenovic et al. 2000) that result in different projections of SLR due to thermal expansion and ice melt over the coming century and beyond. Estimates of thermal expansion impacts on eustatic SLR were based on the range of the coupled Atmosphere-

Table 4 Recurrence intervals (T_r) for storm surge anomaly heights associated with some major storms for Boston, Massachusetts and Atlantic City, New Jersey, USA

Event	Event date	Anomaly height (mm)	T_r (event year)[a]	T_r (2005)[b]
For Boston station				
Perfect Storm	10/31/1991	1,510	>1,000	200–500
Blizzard of 1978	2/7/1978	1,327[c]	10–20	5–10
1993 Superstorm	3/13/1993	1,258	2–5	2–5
Hurricane Gloria	9/27/1985	673	<2	<2
Ash Wednesday storm	3/7/1962	661	<2	<2
Hurricane Donna	9/12/1960	622	<2	<2
Hurricane Floyd	9/17/1999	521	<2	<2
Hurricane of 1938	9/21/1938	394	<2	<2
For Atlantic City station				
Ash Wednesday storm	3/6/1962	1,088[c]	10–20	2–5

Recurrence intervals in the year that the event occurred (T_r event year) were computed by adding in the linear trend from the beginning of the record to the year of the event. For example, the linear trend over 71 years was added to the detrended anomaly height estimates to obtain storm surge anomaly height estimates for Boston in 1991, the year of the "Perfect Storm".

[a] Recurrence interval in the year the event occurred

[b] Recurrence interval in 2005

[c] Annual maximum storm surge anomaly height

Ocean General Circulation Models (AOGCM) used in the IPCC Fourth Assessment Report for which gridded SLR output fields were available. Ice melt impacts were provided by Hayhoe (personal communication 2006) using the Model for the Assessment of Greenhouse-Gas Induced Climate Change (MAGICC, Wigley 1994) framework. For a lower emissions scenario, SRES B1, an eustatic global SLR by the end of the century ranging from approximately 10 to 60 cm relative to the present day was found. In contrast the higher emissions scenario, SRES A1fi, projects SLR of approximately 20 to 90 cm by the end of the century as the oceans absorb more heat and ice sheets melt more rapidly. For our analysis, the lowest projection of the B1 range and the highest of the A1fi range were used to provide the widest envelope of possibilities. The eustatic SLR scenarios are shown in Fig. 3.[1]

It should be noted, however, that the ice melt estimates used here are conservative and others such as Rahmstorf (2007) state higher rates are certainly possible. This seems reasonable given the recent observations of rapid ice melt on Greenland and the West Antarctic Ice Shield.

The estimates of future local and eustatic SLR were then added to the storm surge anomaly quantiles, yielding future storm surge heights likely to occur under higher and lower emissions scenarios.

[1] The Kirshen et al. analysis, which preceded the release of SLR projections by the IPCC AR4 Summary for Policy Makers, WG1 report (AR4), used projections of sea level rise due to thermal expansion based on simulations by a range of IPCC AR4 models, combined with estimates of SLR due to ice melt based on MAGICC simulations tuned to reproduce the SLR range provided in the IPCC Third Assessment Report (2001). The 12 cm value used in this analysis for the lower B1 scenario is less than the lower B1 value of 18 cm reported in AR4. The 86 cm value used here is greater than the higher A1 fi value of 59 cm reported in AR4, but less than the mid-range A1 fi value provided by Rahmstorf (2007) of 95 cm. An updated analysis of coastal flooding by Kirshen et al. uses the IPCC AR4 SLR projections. These results are presented in the synthesis report of the Northeast Climate Impacts Assessment. A description of the updated data and methods is available at: www.northeastclimateimpacts.org

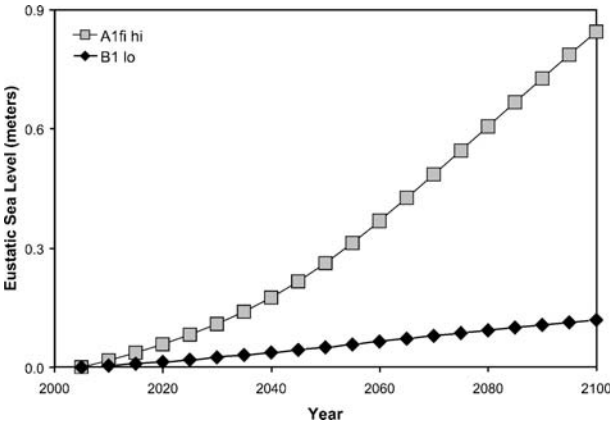

Fig. 3 Estimated increase in eustatic sea levels under the lowest of the lower emissions scenarios (B1 lo; *black diamonds*) and the highest of the higher emissions scenarios (A1fi hi; *grey squares*)

The last step in this process was to add in the tidal component so that storm surge heights could be converted to water level elevations. To be conservative, we used mean higher high water (MHHW, the average of the higher high water height of each tidal day, US Department of Commerce 2000) to represent tide height. The difference between MHHW and mean sea level (MSL) relative to NAVD was used to represent the tidal height and was added to the storm surge heights computed for each station to estimate the stillwater elevations. Wave runup elevation impacts were not included even though they can be significant along the coastline.

As an example of the detailed results, the recurrence intervals of future flooding are given in Fig. 4a (detrended anomalies) and Fig. 4b (raw anomalies) for Boston. Table 5 gives the magnitudes of 100-year flood elevations at the five sites for 2005, 2050, and 2100. In addition, Table 5 presents the recurrence intervals of the 2005 100-year flood in the future. For example, the elevation of the 2005 100-year flood in New York City has a recurrence interval of 50 years under the B1 lower SLR scenario. To illustrate in more detail

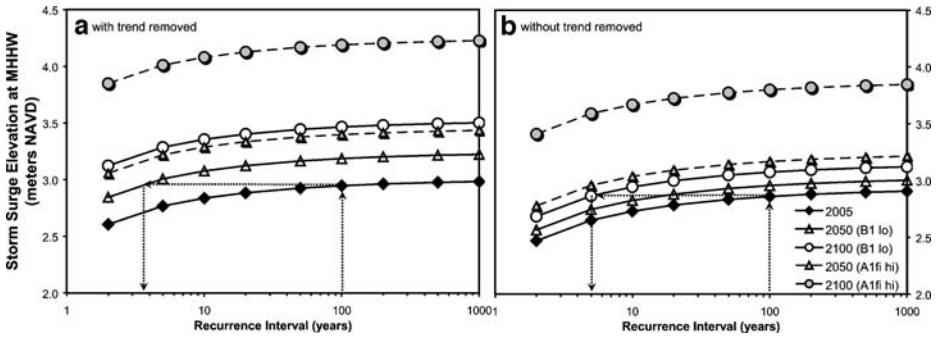

Fig. 4 Projected storm surge elevations (in meters relative to the North American Vertical Datum of 1988 [NAVD]) by recurrence interval for 2005 through 2100 for Boston, Massachusetts, USA for: **a** with trend removed prior to frequency analysis; and **b** without trend removal prior to frequency analysis. *Black diamonds* represent storm surge elevations in 2005. *Open symbols* represent the lower emissions scenario (B1 lo) and *filled symbols* represent the higher (A1fi hi) scenario. The *dashed line* illustrates how the recurrence interval of the 2005 100-year storm surge elevation is dramatically reduced in the future scenarios

Table 5 Estimated storm surge elevations for 2005, 2050 and 2100 for each site

Station	100-year storm surge elevation			Recurrence interval of 2005 100-year Anomaly (years)	
	At MHHW (meters NAVD)				
	2005	2050	2100	2050	2100
Boston- B1 lo (trend removed)	3.0	3.2	3.5	3	≪ 2
Boston—A1fi hi (trend removed)	3.0	3.4	4.2	≪ 2	≪ 2
Boston—B1 lo (trend not removed)	2.9	3.0	3.1	15	5
Boston—A1fi hi (trend not removed)	2.9	3.2	3.8	3	≪ 2
Woods Hole—B1 lo	3.0	3.1	3.3	50	35
Woods Hole—A1fi hi	3.0	3.3	4.0	25	≪ 2
New London—B1 lo	2.2	2.3	2.4	70	50
New London—A1fi hi	2.2	2.3	3.1	30	3
New York City—B1 lo	2.8	2.9	3.0	50	30
New York City—A1fi hi	2.8	3.1	3.7	30	3
Atlantic City—B1 lo (trend removed)	2.4	2.8	3.4	6	≪ 2
Atlantic City—A1fi hi (trend removed)	2.4	3.1	4.1	2	≪ 2
Atlantic City—B1 lo (trend not removed)	2.2	2.3	2.5	30	10
Atlantic City—A1fi hi (trend not removed)	2.2	2.5	3.2	8	≪ 2

Also included are the recurrence intervals in 2050 and 2100 for the 2005 100-year storm surge elevation. Estimates with and without trend removal prior to frequency analysis are included for Boston, Massachusetts and Atlantic City, New Jersey, USA.

the socio-economic impacts at one station, these heights were registered to a high resolution digital elevation model of metropolitan Boston to develop coastal flooding and inundation maps. Inundation maps were developed for 2005 and compared to coastal flooding maps developed by FEMA. Inundation maps were also developed for 2100. Results are shown in Fig. 5a and b.

3 Results

Table 5 shows that, while the impacts of climate change and local SLR vary by site, the frequency of extreme storm surge events will increase at all sites by 2050. Under the higher emissions scenario (A1fi), the 2005 100-year storm surge event will recur at the very least once every 30 years (on average) at US each station. Boston, Massachusetts and Atlantic City, New Jersey will be impacted the most with new recurrence intervals of less than 8 years. Under the lower emissions scenario (B1), by 2050, the flood elevation of the 2005 100-year storm surge event will occur at least once every 70 years at all sites. At Boston and Atlantic City, the frequency of this event could be increased to once every 30 years or less.

Site specific impacts include:

Boston, Massachusetts, appears particularly susceptible to relative SLR changes. Under both emissions scenarios, by 2050 the 100-year storm surge will exceed the elevation of the 2005 1,000-year storm surge and the recurrence interval of the 2005 100-year storm surge will be less than 15 years. This result is sensitive to the choice of

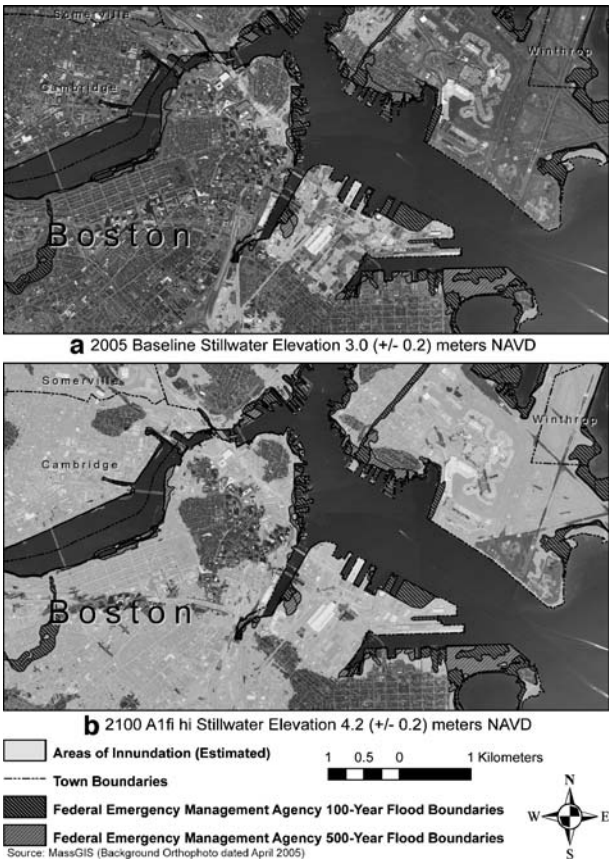

Fig. 5 Estimated storm surge inundation areas (not including wave action) for Boston, Massachusetts, USA Inner Harbor with trend removal (elevations shown in Fig. 4) for: **a** 2005, overlain with current Federal Emergency Management Agency (FEMA) inundation boundaries; and **b** 2100 under the higher (A1fi hi) emissions scenario

raw or detrended data analysis and to emissions scenario. The impacts are more substantial under the higher Alfi scenario, especially when the trends are removed. Figure 5a shows the coastal floodplain mapped by FEMA for parts of Boston, Massachusetts, superimposed on an aerial photo. It also shows the 2005 100-year storm surge floodplain based upon our stillwater analysis. It includes additional areas inland of the FEMA floodplain as well as the FEMA floodplain. Figure 5b is the same as Fig. 5a except that it shows the extent of the stillwater flooding of a 100-year storm surge event in 2100 under the higher emissions A1fi scenario with the trend removed. Figure 5b shows that the additional sea-level rise leads to considerably more flooding of highly developed areas, including areas upstream of the Charles River Dam as well as the region's major airport, Logan International Airport in Boston.

In **Woods Hole**, Massachusetts, by 2050, as shown in Table 5, the recurrence interval of the present 100-year storm surge will be less than 50 years under the lower emissions scenario, and 35 years or less by 2100. Under the higher emissions scenario the changes are 25 years in 2050 and less than every 2 years in 2100.

In **New London, Connecticut, and New York, New York**, in 2100, the 2005 100-year flood will have a recurrence interval of 3 years under the higher emissions scenario. Recurrence intervals in 2100 of the 2005 100-year flood event under the lower emissions scenario will be 50 years for New London and 30 years for New York.

The range of changes in the 100-year storm surge elevations in the future is similar to that of Rosenzweig and Solecki (2001) even though they used different emissions scenarios and climate models.

Atlantic City, New Jersey, is also very susceptible to relative SLR change with results being sensitive to the choice of emissions scenario. For example, under the lower emissions scenario with the trends not removed, the recurrence interval of the 2005 100-year storm surge event in 2100 is 10 years, but under the higher emissions scenario the recurrence interval is less than 2 years. Significant differences also exist for the recurrence intervals of the 2005 100-year event in 2050 depending upon the emissions scenario. The range in the elevation increases in storm surge elevations is similar to that found by Cooper et al. (2005) for New Jersey.

4 Conclusions

We analyzed historical sea level information for storm surge anomalies at five sites in the northeastern United States using state-of-the-art statistical techniques. The impacts of climate change and local sea level effects were then added to this analysis. We found that climate change-driven sea level rise will lead to significant elevation increases in storm surges by at least 2050 at all locations but particularly at Boston, Massachusetts and Atlantic City. The difference in storm surge height widens over the rest of the 21st century depending on whether a higher or lower emissions pathway is followed in the future. While the results do not fundamentally change with additional detrending of the data for Boston and Atlantic City, New Jersey, further research is needed to determine the cause of the trend in anomalies at these locations and to determine the vulnerabilities of all of the coastal areas to these elevation changes. Based on previous storm surge damages in the region, the economic and environmental damages associated with these changes will be severe.

Acknowledgements The authors appreciate the support of the other participants in the Northeast Climate Impacts Assessment (NECIA) sponsored by the Union of Concerned Scientists. We are particularly grateful to Katharine Hayhoe for providing the SLR scenarios and the NECIA Synthesis Team and the article reviewers for their comments. Richard Vogel provided useful statistical insights. We are also grateful to Elisabeth Militz and Rita Koros who acquired the sea level data. Cameron Wake and Susi Moser provided leadership in assembling this article.

Appendix A: GEV frequency analysis

For large samples, the cumulative distribution function for the maximum values of many probability distributions converges to one of three extreme value distributions (EV type I, II, or III) described by Gumbel (1958). The Generalized Extreme Value (GEV) distribution is a general mathematical form which incorporates Gumbel's type I, II and III distributions for maxima (Stedinger et al. 1993). The parameters of the GEV distribution are ξ (location parameter), α (scale parameter) and κ (shape parameter). The Gumbel (EV type I) is obtained when κ=0. For κ>0, the distribution has a finite upper bound at $\xi + \alpha/\kappa$ and corresponds to the EV type III distribution for maxima that are bounded from above. For this study, GEV parameters were estimated using the method of L-moments (Stedinger et al. 1993; Hosking and Wallis, 1997) and are shown in Table 6. GEV goodness-of-fit was

Table 6 GEV parameters estimated using the method of L-moments, following Hosking and Wallis (1997)

GEV parameters[a]	Boston[b]	Boston[c]	Woods Hole	New London	New York City	Altantic City[b]	Altantic City[c]
ξ	0.937	−0.054	0.698	0.759	0.935	0.690	−0.097
α	0.236	0.219	0.157	0.224	0.260	0.285	0.178
κ	0.434	0.465	−0.079	−0.034	0.030	0.198	0.031

[a] GEV parameters estimated from anomaly data in units of meters and later converted to mm.

[b] Linear trend was not removed prior to estimating GEV parameters.

[c] Linear trend was removed prior to estimating GEV parameters.

confirmed using a probability plot correlation coefficient (PPCC) hypothesis test (Chowdhury et al. 1991) and an *L*-moment diagram. The PPCC hypothesis test indicated that the GEV adequately fit the annual maximum time series for all sites except Boston. However, the *L*-moment diagram indicated that the GEV could reproduce the moments of the detrended Boston data. In addition, a visual inspection of PPCC plots (Fig. 6) showed that the GEV fit the upper tail of the Boston time series reasonably well after the largest (1991) data point was removed; hence the GEV was deemed appropriate for all sites. For the Atlantic City and Boston sites, parameters were estimated both with and without trend removal.

Using the parameters estimates in Table 6, GEV quantile estimates, x_p, for specified cumulative probabilities, p, were computed from

$$x_p = \xi + \frac{\alpha}{\kappa}\{1 - [-\ln(p)]^{\kappa}\} \qquad (A-1)$$

Cumulative probabilities (p) were converted to exceedance probabilities, $p_e = 1 - p$. The return periods shown in Table 3 are $1/p_e$.

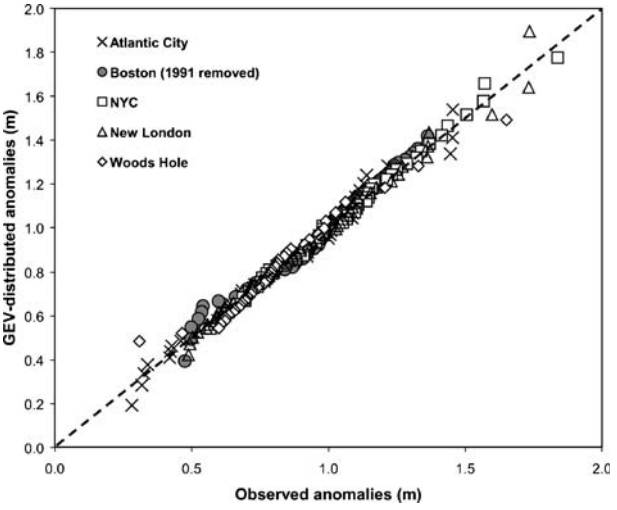

Fig. 6 Probability plot correlation coefficient (PPCC) plots for annual maximum time series. The Generalized Extreme Value (GEV) distribution was selected based on the results of the PPCC test and L-moment diagrams

References

Bindoff N, Willebrand J (2007) Chapter 5: Observations: oceanic climate change and sea level. In: Solomon S, Dahe Q, Manning M (eds) Climate change 2007: the physical science basis. Cambridge University Press, Cambridge, U.K

Chowdhury JU, Stedinger JR, Lu L-H (1991) Goodness-of-fit tests for regional generalized extreme value flood distributions. Water Resour Res 27(7):1765–1776

Church JA, Gregory JM (2001) Chapter 11: changes in sea level. In: Houghton JT et al. (eds) Climate change 2001: the scientific basis, third assessment report. Cambridge University Press, Cambridge, U.K., pp 639–694

Church JA, White NJ, Coleman R, Lambeck K, Mitrovica JX (2004) Estimates of the regional distribution of sea level rise over the 1950–2000 period. J Clim 17:2609–2625

Clark G, Moser S, Ratick S, Dow K, Meyer M, Emani S, Jin W, Kasperson J, Kasperson R, Schwarz H (1998) Assessing the vulnerability of coastal communities to extreme storms: the case of Revere, MA, USA. Mitig Adapt Strategies Glob Chang 3:59–82

Cooper M, Beevers M, Oppenheimer M (2005) Future sea level rise and the New Jersey Coast, assessing potential impacts and opportunities. Woodrow Wilson School of Public and International Affairs. Princeton University, Princeton, NJ

Douglas, EM, Vogel RM (2006) The behavior of the flood of record for basins in the U.S. J Hydrol Eng 11 (5):482–488

Emanuel KA (2005) Increasing destructiveness of tropical cyclones over the past 30 fears. Nature 436:686–688

Flather R, Williams J (2000) Climate change effects on storm surges: methodologies and results, ECLAT-2 Report No 3. Climatic Research Unit, University of East Anglia, Norwich, UK

Flick R, Murray J, Ewing L (1999) Trends in United States tidal datum statistics and tide range, a data atlas report. Scripps Institute of Oceanography Reference Series Number 99–20, December, 1999

Gumbel EJ (1958) Statistics of extremes. Columbia University Press, New York

Holgate S J and Woodworth PL (2004) Evidence for enhanced coastal sea level rise during the 1990s. Geophys. Res. Ltrs, 31, L07305, DOI 10.1029/2004GL019626

Hosking JRM, Wallis JR (1997) Regional frequency analysis: an approach based on L-moments. Cambridge University Press, Cambridge, U.K

Kirshen P, Ruth M, Anderson W and Lakshmanan TR (2004) Infrastructure systems, services and climate change: integrated impacts and response strategies for the Boston metropolitan area. Final Report to US EPA ORD, EPA Grant Number: R.827450–01

Kirshen P, Ruth M, and Anderson W (2006) Climate's long-term impacts on urban infrastructures and services: the case of Metro Boston, Chapter 7 of Ruth M, Donaghy K, and Kirshen PH, (eds.) Climate change and variability: local impacts and responses. Edward Elgar Publishers, Cheltenham, England

Nakicenovic N, Alcamo J, Davis G et al. (2000) IPCC Special report on emissions scenarios. Cambridge University Press, Cambridge, United Kingdom

New England Regional Assessment Group (2001) Preparing for a changing climate: the potential consequences of climate variability and change. New England Regional Overview, U.S. Global Change Research Program, University of New Hampshire, Durham NH, 96 pp

NOAA (2007) National Oceanic and Atmospheric Administration, Center for Operational Oceanographic Products and Services, Tides and Currents. http://tidesandcurrents.noaa.gov/. Cited 17 May 2007

Nucci Vine Associates, Inc. (1992) Potential effects of sea level rise in Boston Inner Harbor. Newburyport, Massachusetts, 36 pp

Pugh D (2004) Changing sea levels: effects of tides, weather and climate. Cambridge University Press, Cambridge, United Kingdom

Rahmstorf, S (2007). A semi-empirical approach to projecting future sea-level rise, Science, Vol 315, 19 January

Rosenzweig C, Solecki W (eds) (2001) Climate change and a global city: the potential consequences of climate variability and change—Metro East Coast. Report for the US National Assessment of the Potential Consequences of Climate Variability and Change, Columbia Earth Institute, New York

Stedinger, JR, Vogel RM, Foufoula-Georgiou E (1993) Frequency analysis of extreme events. In: DR Maidment (ed) Handbook of Hydrology. McGraw-Hill, Inc., New York, pp 18.1–18.66

Thompson EM, Baise LG, Vogel RM (2007) A global index earthquake approach to probabilistic assessment of extremes. J Geophys Res 112, B06314, DOI 10.1029/2006JB004543

US Army Corps of Engineers (1990) Flood damage reduction, main report, Saugus river and tributaries. New England Division, Concord, Massachusetts

US Department of Commerce (2000) Tide and current glossary. Silver Spring, Maryland

van den Brink HW, Konnen GP, Opsteegh JD (2003) The reliability of extreme surge levels estimated from observational records of order hundred years. J Coast Res 19(2):376–388

Wigley TML (1994) MAGICC (Model for the Assessment of Greenhouse-Gas Induced Climate Change): user's manual and scientific reference manual. National Center for Atmospheric Research, Boulder, Colorado

Zhang K, Douglas B, Leatherman SP (2000) Twentieth-century storm activity along the U.S. East Coast. J Climate 13:1748–1761